BENCHMARKING OF THE 3D CFD CODE GASFLOW II WITH CONTAINMENT THERMAL HYDRAULIC TESTS FROM HDR AND THAI

P. Royl, U. J. Lee[1], J. R. Travis, W. Breitung
Forschungszentrum Karlsruhe
Institut für Kern- und Energietechnik
Box 3640, D76021 Karlsruhe, Germany
[1] Korea Atomic Energy Research Institute,
P.O.Box 105, Yuseong, Daejeon, 305-600, Korea

Abstract

A good understanding of the thermal hydraulic conditions resulting from steam-hydrogen releases in nuclear reactor containments is required for all aspects of accident management and for the design of mitigation measures. The GASFLOW II code has been developed at Forschungszentrum Karlsruhe (FZK) for analysis of such scenarios. It solves the three dimensional compressible transient Navier Stokes equations. This contribution will report on new validations of GASFLOW II with blind and open post-test simulations of experiments that simulate such conditions in the new ThAI containment test facility and in the Heissdampfreaktor (HDR) in Germany.

Introduction

Severe accidents in pressurized water reactors can lead to the release of steam and hydrogen and build up sensitive mixtures in the containment with a combustion potential to develop thermal and mechanical loads. The resulting thermal hydraulic conditions can be strongly three dimensional. A good understanding of these conditions is required for all aspects of accident management and for the design of mitigation measures. The GASFLOW II code has been developed at FZK [1] for analysis of such scenarios. It solves the three dimensional compressible transient Navier Stokes equations. GASFLOW is used already since some time to simulate such severe accident sequences in nuclear reactor containments. It has been validated with analysis of various experiments that study transient steam-hydrogen distributions with/without mitigation by catalytic recombiners in complex geometries [2]. Further code validations with experiments performed in the new German ThAI facility are available now. This facility was built with funding from the German Bundesministerium für Wirtschaft und Arbeit and is operated by Becker-Technologies. Successful GASFLOW validations with the ThAI tests TH1 and TH7 with only steam release into air have been published [3]. The ThAI tests TH10 and TH13 which involved the release of both steam and Helium as a simulator for hydrogen have meanwhile also been analyzed with GASFLOW.

Test TH10 simulated the sequence of thermal hydraulic processes that occurred in the integral HDR test E11.2 [4] on a smaller scale under well controlled boundary conditions with better instrumentation. Test E11.2 is a full scale experiment that was performed in 1989 in the German Heissdampfreaktor (HDR) Containment. It was defined as an international standard problem (ISP22) . Its results have often been questioned in the past after no code was able to blindly predict the measured distribution of the light gas mixture of hydrogen and helium that simulated the hydrogen in this test. The CFD post test simulation of this test with GASFLOW could interprete it already quite well in 1996 [5]. The recent test TH10 confirmed the findings from this early test E11.2 also for the smaller scale of the ThAI facility. We have blindly calculated this experiment with GASFLOW, submitted our results to Becker Technologies and in return received the test data for validating our code [6]. We then performed post test analyses and further improved our prediction and those from our earlier GASFLOW analysis of the HDR test E11.2. The ThAI test TH13 was performed as last step in a series of experiments in the new containment test facilities, TOSQAN, MISTRA from France, and ThAI from Germany. It is part of an international code benchmark organized by the OECD in the frame of a new international standard problem (ISP47) and was analyzed by different users of CFD and also coupled volume (lumped parameter=LP) codes.

This contribution will report on the blind pre-test and open post-test GASFLOW calculations performed for the tests TH10 and TH13 and it will discuss the results from the re-analysis of test E11.2 with the new findings from the interpretation of test TH10.

ThAI Test TH10

The ThAI facility (figure 1) has a cylindrical steel vessel of 60 m3 volume, 3.2 m diameter, and 9.2 m height. It is insulated with a thick layer of rock wool on the outside, has a central inner cylinder of 1.26 m diameter, which is open at the lower end and partially open at the top and has 2 condensate

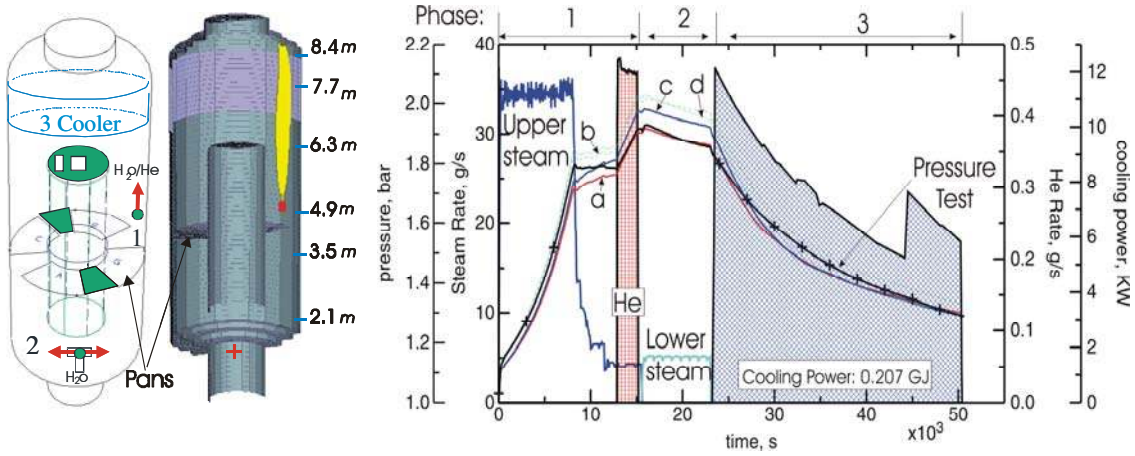

Figure 1:Test conditions of ThAI test TH10 with calculated pressures from different GASFLOW simulations

trays of 150 degrees each that are distributed around the mid part on the outside of the cylinder. They divide the annulus around the inner cylinder and leave open a slit of 30 degrees on each side for communication between the upper and lower region of the annulus. The arrangement for test TH10 had a 180 degree symmetry. Test TH10 simulated a small break LOCA scenario with a high release location. Figure 1 summarizes the test conditions. Phase 1 (duration 15000 s) started from air at atmospheric conditions and room temperature with an eccentric axial steam injection with a high rate of 35 g/s during the first 9000 s. Helium (1kg) is mixed into the steam jet during the last 2000 s in a source gas mixture with 50 Vol % steam. Phase 2 (duration 8000 s) had a radial steam injection at a low location from an impingement plate in the center with a weak injection momentum. As in the early test E11.2 the objective of the late steam release at the low location was to investigate the possibility to break up the stratified He/steam layer resulting from phase 1. Phase 3 (duration 27,000 s) started at 23,000 s. It simulated the outside spray cooling in the HDR test E11.2 by activating the upper cooler blanket of the facility. Measured flow rates and inlet and outlet temperatures of the cooling oil from this blanket defined the transient cooling power, that is quite homogeneously removed in the displayed cooler region. The total test duration was 14 h. The vessel structure was defined in GASFLOW as stair stepped obstacles that filled fluid cells. The obstacles for the vessel structure and the boundary of the mesh were simulated as slabs of a composite material from steel, oil, and rock wool with a convective heat transfer from the rock wool to the outside room where air was assumed at a constant temperature of 298 K. The 1D heat conduction model in GASFLOW for each structure element applied a nodalization with 40 nodes that was fine enough to simulate the vessel with the multi layer structure of steel, oil, and rock wool on the outside and determine the inner vessel surface temperature as reference for the heat transfer and condensation. We defined a special material for the cooler blanket and released the measured cooling power in the oil region of the structure.

Table 1: GASFLOW simulations of ThAI test TH10

Case		Mesh	Advection scheme	360°Axial Inj.Area [cm^2]	Comment
a	red	I	Donor Cell	124	blind
b	gr. dashed	II	Donor Cell	15.4	-
c	blue	III	Van Leer	15.4	-
d	light blue	IV	Van Leer	172	-

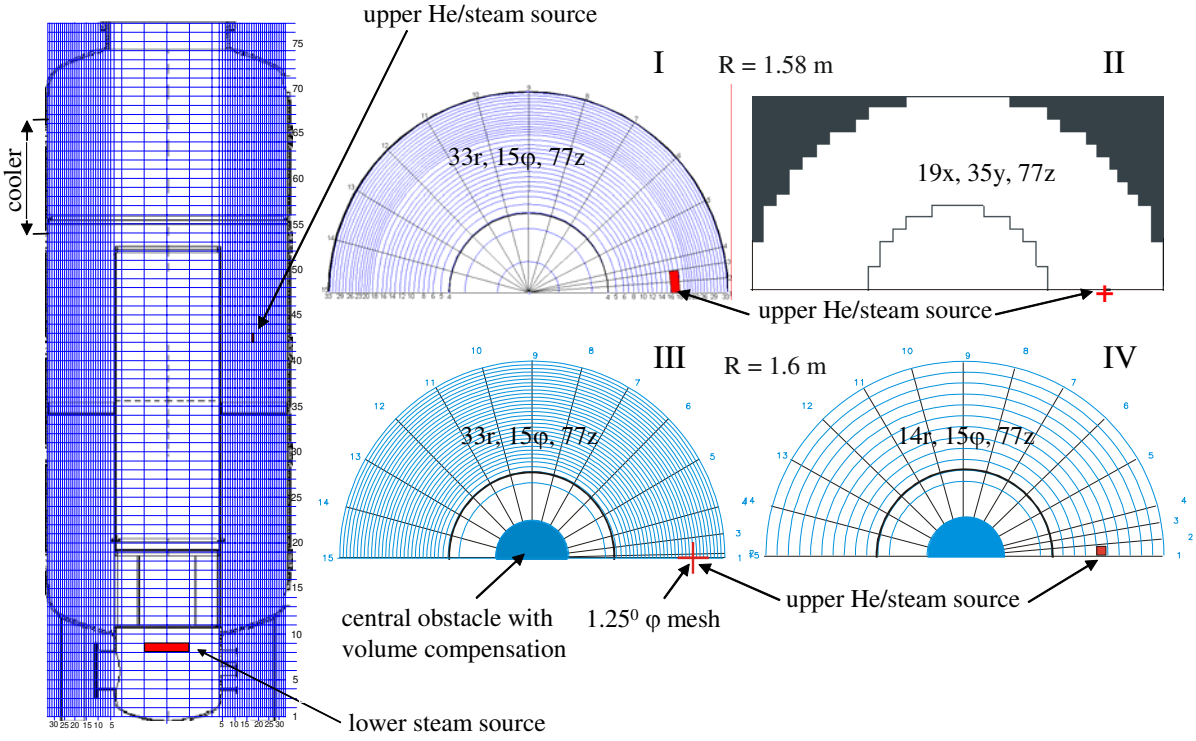

Figure 2:GASFLOW meshes for modelling the ThAI facility in test TH10

Table 1 lists the four GASFLOW simulations that were performed for this experiment with the different meshes shown in fig. 2. All simulations modeled a 180 degree segment of the facility using a structured orthogonal mesh with cylindrical, in one case also cartesian coordinates. GASFLOW uses a staggered mesh and applies the so called ALE (Arbitrary Lagrangian Eulerian) integration scheme. Integration over one time step is done in three steps. Phase A simulates a Lagrangian extrapolation of all primitive dependent mesh variables. Phase B, the pressure iteration phase, simultaneously solves for all primitive variables from phase A to the same time level. Phase C maps back the expanded mesh to the fixed Eulerian mesh. Different advection schemes can be applied in Phase C. The standard solution algorithm with donor cell advection was applied in the blind analysis case a and in case b with the Cartesian mesh. Cases c and d applied the second order van Leer advection scheme for the remapping of the Lagrangian variables. GASFLOW simulates the gas injection during the test by defining certain cells at appropriate positions in the mesh as source reservoirs with time dependent compositions that reflect the upper and lower gas injections. The reservoirs are sealed off by walls from the remainder of the mesh and have open faces in the direction of the injection. Material is injected into the test vessel from these reservoirs by specifying corresponding velocity boundary conditions that represent the time dependent injection rates from fig. 1. The real cross section of the axial injection nozzle (15cm2) could not be simulated in mesh I at the location for the axial injection. Thus the momentum of the vertical jet with an injection velocity of 30 m/s during the first 9000 s could not be represented in the blind simulation. To avoid severe time step cuts from the Courant limitation and extensive computation times with the explicit convection model in GASFLOW, we distributed the axial jet at the high injection point over an 8 times larger injection area and injected from two cells with a total injection area of 124 cm2 in our blind analysis. Earlier analysis showed that the injection momentum plays a minor role during the vertical injection of a buoyant gas because it is quickly outweighed by the acceleration from the buoyancy. But during the long period of upper steam injection in test TH10 it turned out that a steam volume fraction of nearly 70% developed above the injection nozzle which should give more importance to the real injection momentum in the later phase of the upper steam

injection after 9000s. All 3D simulations applied the standard k-ε turbulence model from GASFLOW and evaluate heat, mass and momentum transfer with the built in wall functions for forced flow with no-slip conditions.

The pressure from the blind analysis (case a) agrees quite well with the test data that are marked with black crosses in fig. 1. In spite of the ongoing injection GASFLOW predicts a slow pressure de-

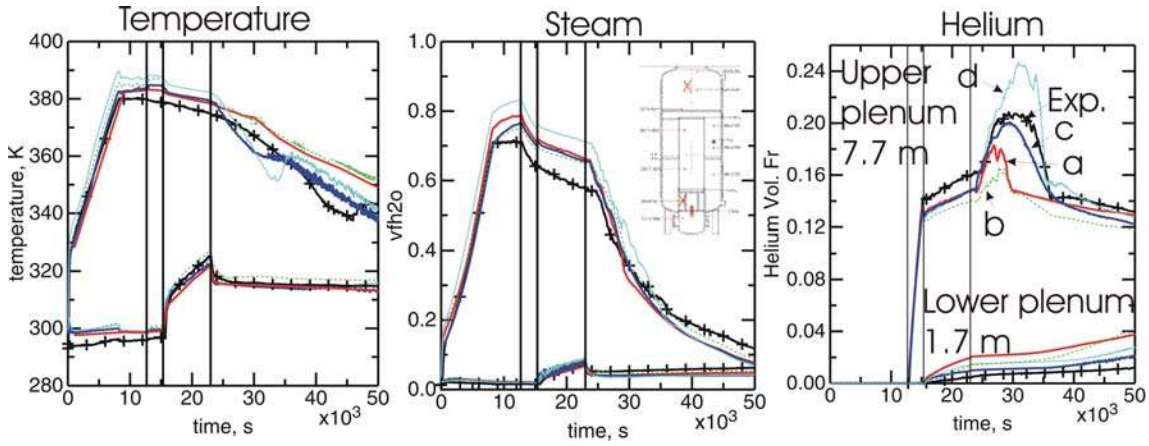

Figure 3: Temperatures, steam- and Helium volume fractions in test TH10

cay in phase 2 which is also in excellent agreement with the test data. The steam temperature and volume fraction in the dome (fig. 3) follow the test data quite well initially. But already shortly before the decay of the steam injection rate at 9000 s they exceed the test data and they stay at a higher than measured level up to the activation of the cooler jacket after 23,000 s. Excellent agreement with the sensor data is seen at the 1.7 m level for the whole experiment. The Helium concentration in the dome is well predicted when only looking at the initially measured dry helium concentration without steam. But fig. 3 compares the wet Helium concentration in the mixture with steam and air. It is a little lower in GASFLOW which is a result of the early over prediction of the steam concentration in the dome. But the stable stratified region is well predicted. The increase of the Helium volume fraction in the dome during the lower steam injection in phase 2 is a result of the ongoing steam condensation in the dome. In this phase the lower heavier steam air cloud gradually moves up the upper Helium steam air cloud like a piston to replace the condensed steam volume in the dome. The rapid steam condensation after the activation of the cooling jacket in phase 3 triggers a much stronger increase in the Helium volume fraction. This tendency is well predicted in GASFLOW. The steam condensation that increases the Helium volume fraction induces a secondary flow near the wall that is shown in fig. 4. This condensation induced near wall convection is

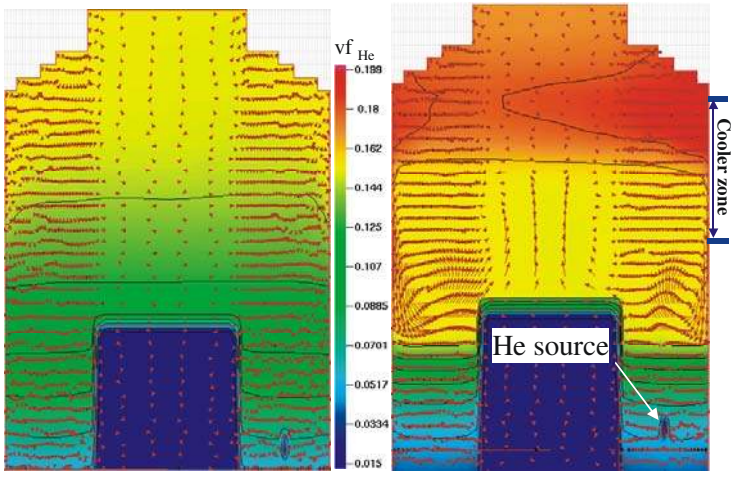

Figure 4: Impact of cooler activation on Helium volume fraction and flow field in upper plenum for case a

important for containment applications. It can only be predicted in a CFD approach. It mixes the atmosphere and transports a generally heavier Helium-air-steam mixture into the lower part of the containment. We call this process condensation sedimentation because the dried Helium-air mixture near the wall has a higher macroscopic density for most containment conditions. Figure 5 gives the results from a thought experiment that explains the sedimentation effect of the local density changes from steam condensation near the wall. It is only when the wet Helium concentration is above a certain threshold that the density of the dried gas with a higher Helium volume fraction gets smaller so that the dried gas can rise. In most cases its density is higher and a secondary downward convection develops along the condensing wall that brings the hydrogen (Helium) gas into the lower containment region. The map in fig. 5 gives the threshold for sedimentation/stratification for all wet mixtures of steam/hydrogen(Helium)/air. Conditions from various experiments are marked in this map. As an example, assume a wet atmosphere with 50% steam, 20% hydrogen and 30% air. A mixture with 40% hydrogen and 60% air develops when totally condensing the steam. The red line shows the limits for the dry density equaling the wet density. Any wet mixture with a lower hydrogen content will locally have a higher density from steam condensation and sink. The Helium volume fraction from the blind analysis in fig. 3 increases to a peak of 18%.before it is homogenized by the near wall convection. The test data show a Helium peak of 22% in the dome. The homogenization from the near wall convection occurs later. GASFLOW predicts the homogenization too fast in the blind calculation but then gives the correct Helium concentration in the upper cloud with the homogenized atmosphere.

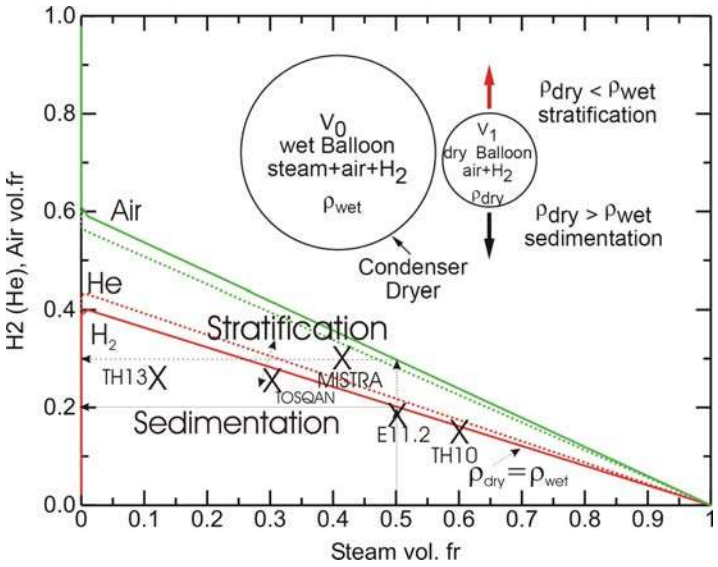

Figure 5: Thought experiment on local density changes during steam condensation from hydrogen (Helium), air, steam mixtures

Post test calculations cases b, c, and d were run to improve the shortcomings seen in the blind analysis. We attribute the over prediction of the steam concentration and gas temperature in phase 1 to an under prediction of the air entrainment with the rising steam, that was injected with a too low momentum in our blind calculation. Case b simulated the correct injection momentum and used a source cell with the correct face area of 15 cm2. This was not directly possible with the cylindrical model from the blind simulation. Using a small azimuthal angle of 1.25 degrees for the first angular mesh was necessary to achieve the correct face area of the source cell. But this cut down the time step to less than 1.e-4 s, which made it impossible to analyze phase 1. The criterion was not the material Courant condition, the built in stability criterion that limits the convection within a time step to less than a cell length. A similar stability criterion is applied in GASFLOW to diffusion processes that also limits the time step due to diffusion velocities to less than a cell length. It was the diffusion enhanced by turbulence that restricted the time step at the midpoint of the central radial and the first azimuthal cell. Mesh I in fig. 2 shows how the already narrow azimuthal travel distance available in the central radial mesh would further reduce when going down from an angular segment of 5 to 1.25 degrees. To avoid

this problem around the central singularity case b applied the Cartesian mesh II from fig.2. The time step was limited then in phase 1 by the material Courant condition from the axial steam jet to 0.7 ms. It became quite small compared to the larger time step for case a of 5 ms that was diffusion controlled. The running time of the calculation with the Cartesian mesh was more than 5 times longer than in case a. The correct injection momentum in case b did reduce the steam concentration in phase 1 through an enhanced air entrainment. But the altered mesh also lead to a higher pressure and gas temperature. The wall functions were applied in case b with larger mesh sizes near the wall which lead to a reduced heat transfer and condensation. Also the stair stepping of the vessel surface (fig. 2) altered the condensation coefficients in the Cartesian mesh significantly. Due to the widely varying free convection conditions along the vessel wall one cannot a priori simulate wall heat transfer and condensation with a wall function developed for forced flow conditions. This is a generic problem for all CFD codes. Its proper solution requires a detailed wall treatment that resolves the boundary layer with a local mesh refinement near the walls. All simulations show the generic tendency of an increased heat transfer and condensation with a reduced wall mesh size which comes from the laminar limit in regions with stagnant flow in which the heat transfer coefficient approaches values that are proportional to the ratio of the thermal conductivity and the half size of the near wall mesh. Note that the distributed structure surfaces and heat capacities used in case b have all been adjusted to be the same as in case a.

Consistent with the higher steam concentration case b gives a wet Helium concentration that is somewhat below the case a results. It shows a similar but weaker increase after the activation of the cooling jacket in phase 3. Case a and b both apply the standard donor cell advection scheme for remapping of the Lagrangian state variables to the fixed Eulerian mesh. Both cases show a steady increase of the Helium volume fraction at the 1.7 m level away from the test data which is an indication for numerical diffusion. We saw already a significant change in case a when activating the van Leer advection in the middle of the run at the start of the Helium injection. Case c investigated this further by consistently applying the 2^{nd} order van Leer advection scheme from the beginning. It applied the cylindrical mesh III in fig. 2 with the first azimuthal mesh reduced to 1.25 degrees to give the correct injection area for the vertical jet. To run this with a feasible time step we put an adiabatic obstacle into the central radial position and compensated for its volume by slightly increasing the axial and radial meshes thus arriving at the same total free gas volume. Phase 1 could thus be analysed with the correct injection momentum and a feasible time step of 1 ms. We used the azimuthal average of all variables in the innermost radial ring at each axial segment to replace the obstacle for displaying the results. Test calculations with and without the central obstacle did not lead to noticeable differences in any of the taken sensor readings during the vertical steam injection. The correct injection momentum from case c enhanced the air entrainment and like in case b lead to smaller steam volume fractions in phase 1. But it also increased the pressure. In case c that used the same near wall mesh the wall heat transfer and condensation should be very similar so that the pressure increase can only come from the applied van Leer advection. It seems that the reduction of the numerical diffusion with the second order scheme causes the pressure increase and that the calculated physical diffusion by molecular transport and turbulence is somewhat too slow in GASFLOW to replace enough of the condensing steam. The predicted temperature in the dome is similar in cases a and c. In case c it drops to nearly the measured values during the cooling phase while in case b it continues to remain at a higher level. The transient Helium concentration from case c during the cooling starts from nearly the same level as in case a. Steam condensation at the coolers then raises it close to the experimental values due to the van Leer advection scheme. There is also a better agreement in the time scale for the atmospheric mixing and the Helium concentration at the 1.7 m level shows results closer to the experimental data. Thus a good agreement of the He prediction with the test data was achieved in case c due to a reduction of numerical diffusion through the application of the van Leer advection scheme

Case d used the coarser mesh IV that was applied in most simulations of test TH13. It simulates the vertical injection with a low momentum and uses the highest injection area of 172 cm2. The coarser mesh allowed a 15 times faster simulation of the whole transient with much larger time steps of 8 ms in phase 1. As expected air entrainment gets smaller and case d gives the highest steam volume fraction from all cases. The temperature in the dome also peaks at the highest values in phase 1. The lower wall heat transfer and condensation resulting from the coarser mesh IV and the reduction of numerical diffusion with the van Leer advection scheme both contribute to the pressure that is the highest from all cases. It looks as if the momentum of the vertical steam injection is of less importance compared to the wall function effect and the reduced numerical diffusion. But due to the higher steam concentration in case d resulting from phase 1 the Helium concentration approaches a too high level during the cooling phase. In the end it levels off to the same homogenized value. The coarse mesh provides probably a sufficient numerical resolution, but in TH10 the injection momentum is no longer negligible in the late part of phase 1 because the steam has a too low buoyancy then.

Recalculation of HDR Test E11.2

As stated earlier the objective of the ThAI test TH10 was the simulation of the HDR test E11.2 under well controlled boundary conditions to better understand its controlling phenomena. We successfully interpreted test E11.2 with GASFLOW in 1996 [5]. Analysis was done with the earlier code version 1 of GASFLOW. Our old GASFLOW analysis is still the only simulation of this experiment with a 3D CFD code. Figure 6 shows the experimental setup, the test conditions, and the

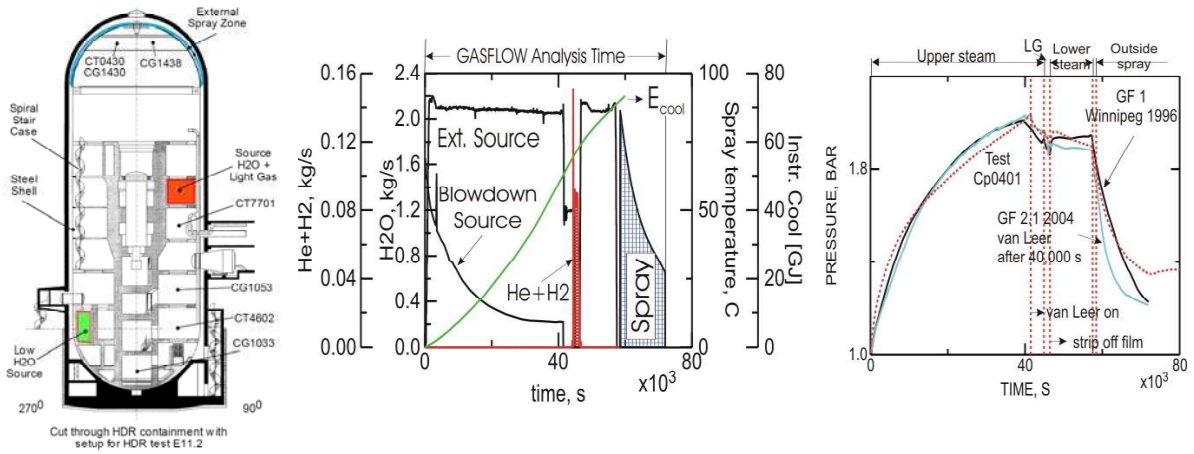

Figure 6: HDR test E11.2 test conditions and pressure from old and new GASFLOW simulation

measured and calculated pressure from the old and the new GASFLOW analysis. Some minor pressure reduction is seen in the new calculation after the upper steam release phase that results from a different film modeling in the current version of GASFLOW. The HDR containment has a height of 60 m, a diameter of 20 m, and a free gas volume of 11,300 m3. Its geometry is quite representative for commercially sized reactor containments. GASFLOW simulated it with a 360 degree cylindrical model of 11 r, 24 φ, and 40 z meshes. The average cell volume for the HDR was 1000 liter compared to about 1 liter for modelling the ThAI facility. The figure shows the high release location (red compartment) for the steam and the light gas (85% He, 15% H2) and the low release location for steam (green compartment). The active cooling was applied as an external spray on the outside of the hemispherical dome (blue zone). The observed time behavior of the light gas concentration in the dome (red curve in fig. 7) is indeed quite similar with what the Helium sensors in the dome region show during the ThAI test

TH10 (compare with fig. 3). The comparison confirms that the objective of test TH10 was fulfilled and that the validity of the old test data for E11.2 can no longer be questioned in view of the test data for TH10. It also demonstrates that an important phenomenon that occurred on a large scale is well simulated on the intermediate scale of the ThAI facility. The GASFLOW 1 analysis from 1996 shows already a steady increase of the light gas concentration during the lower steam release and the strong temporary increase during the outside spray cooling phase peaking at 18% instead of the measured 22%. It is driven by the same mechanisms that control the simulation of TH10. Note also the red cloud with a higher light gas concentration (15 Vol%) on the right. It shows the local increase of the light gas volume fraction near the wall due to steam condensation during the outside spray cooling in the old analysis. The dried red gas is heavier than the core, it sinks and drives the later homogenization like in TH10.

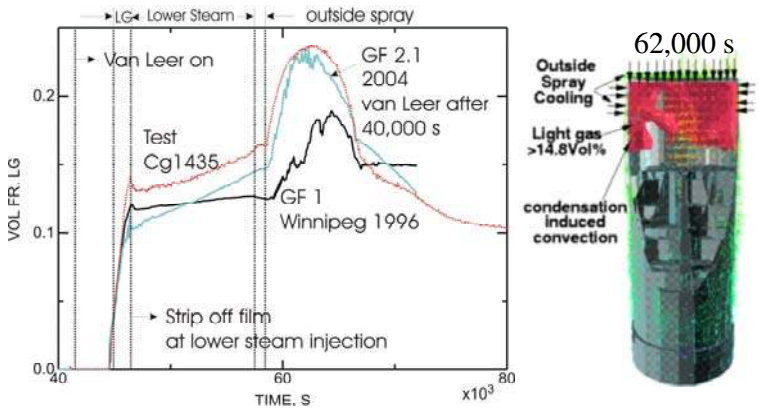

Figure 7: HDR test E11.2, light gas concentration in dome during outside spray cooling, old GASFLOW results with donor cell and new results with van Leer advection

Test E11.2 was re-analyzed with the same GASFLOW version that was used for test TH10. The code runs a lot faster on modern vector machines. While the early E11.2 analysis with GASFLOW 1 took about 4 months of computer time on the older Fujitsu machine from 1996, rerunning this analysis with nearly the same input deck on our modern VPP5000 is now done in one shot and requires only 3 days of CPU for 72,000 s of problem time. The re-analysis used the same input deck, source file, outside spray temperature, and instrument cooling power as the old calculation. The test always had injections against walls or impingement plates that were simulated with volumetric sources of a low momentum. Numerous deflections and mixings occurred while the buoyant source gas penetrated the labyrinth of flow paths to the dome. The injection momentum had no influence on the overall distribution. Using a turbulence model in the coarse mesh for E11.2 which cannot resolve the turbulence had no effect. This is a general finding for all coarse containment models. With the lessons from the analysis of TH10 we activated the van Leer advection scheme at 40,000 s prior to the light gas release in our reanalysis of E11.2. Numerical diffusion obviously came into play also in the old analysis that applied donor cell advection. As in TH10 van Leer advection delays the condensation induced mixing during the outside spray cooling. It leads to a stronger increase of the light gas concentrations during the lower steam release and the outside spray cooling phase and delays atmospheric homogenizations in the dome. Due to the better understanding gained from the analysis of TH10, the new analysis of test E11.2 now gives results which are in even better agreement with the experimental data than the old analysis.

ISP47 ThAI

The ThAI test TH13 was the last of a series of tests that were analyzed as part of the international standard problem ISP47. The basic test setup was the same as for test TH10, but the inner cylinder was fully open at the upper and lower end and there were four instead of two slits with a 30 degree opening angle between the condensate trays that enabled communication between the upper and lower annulus outside the inner cylinder. In this test Helium release preceded the steam release. It started from atmospheric conditions in an air filled test vessel with a uniform temperature of 21 C. Phase I had a vertical Helium injection with 5.6 m/s for 2700 s from an eccentrically located injection nozzle (fig. 8). Phase II had a vertical steam injection with 26 m/s for 2000 s from an eccentric high source that was located on the opposite side of the He nozzle. It was followed by phase III that was designed to have a radial inward steam-injection of 2.7 m/s from an eccentric position 0.42 m below and 0.59m away from the inner cylinder. This injection had the same angular position in the middle between the condensate trays as the vertical steam

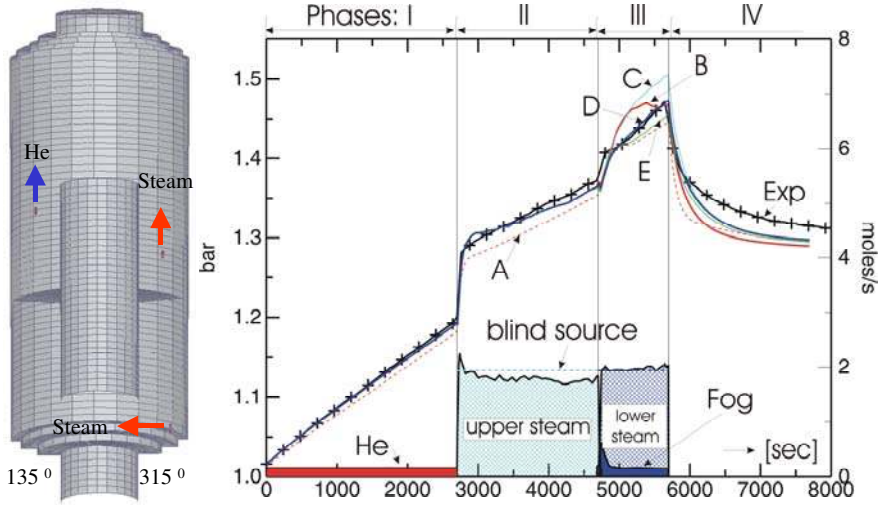

Figure 8: Conditions for ThAI test TH13 with calculated pressures from different GASFLOW simulations

Table 2: GASFLOW simulations of ThAI test TH13

Case		Mesh	360°Axial Inj. Area [cm^2]	360°Radial Inj.Area [cm^2]	Phase III		Comment
					rad. vel.[m/s]	annulus inflow [%]	
A	dashed	I	15.6	144	2.7	23	blind
B	red	II[1]	172	134	2.7	23	-
C	light blue	II	172	278	1.4	81	-
D	blue	II	172	278	1.4	81	plate for asymmetric impingement
E	green	II	172	2502	0.16	100	45 degree source

[1] Axial mesh in source cell for radial injection reduced from 12 to 6.2 cm

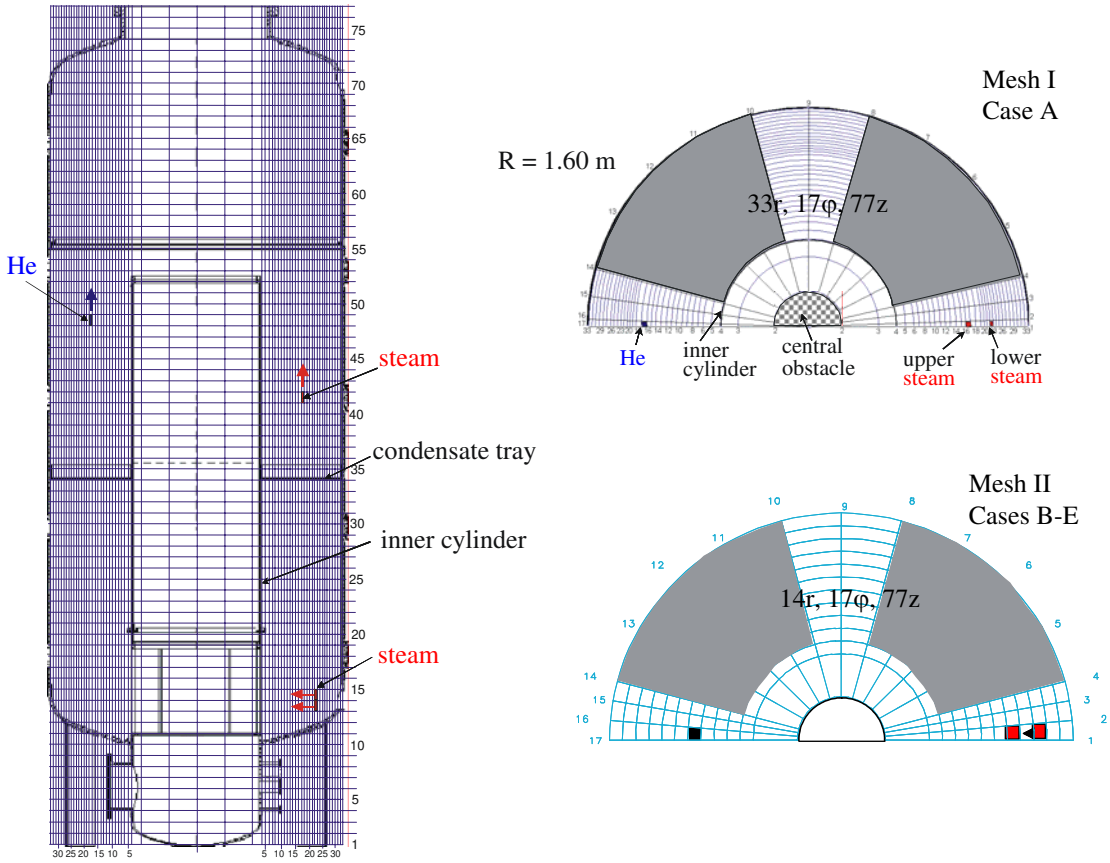

Figure 9: GASFLOW meshes for modelling the ThAI facility in test TH13

injection. Based on measured wall temperatures, it is not clear whether the specified lower steam injection conditions were fully met in phase III. . The available instrumentation shows indications for an asymmetric heating of the vessel below the trays in phase III. Phase IV observed the equilibration after the last injection from 5700 to 7700 s. We have modeled a 180 degree segment of the facility using structured orthogonal meshes in cylindrical coordinates (fig. 9) that were similar to the ones used in the discussed cases c and d for test TH10. Table 2 lists the 5 different GASFLOW simulations for test TH13 which will be discussed below. All simulations for test TH13 used the second order van Leer advection scheme that was also applied in the post calculations of test TH10.

Phases I and II

The mesh sizes were adjusted in the blind case A so that the areas of the feeding faces of the source cells matched the nozzle cross sections. The blind analysis used the pre-specified Helium and steam sources. It could not include the small amount of steam in the Helium that was added to visualize the gas velocities by particle image velocimetry on the fog droplets developing in the source plume. This explains the under prediction of the pressure at the end of phase I. The GASFLOW evaluation of the transport properties of the gas mixture of Helium and air into which steam was injected in phase II gives thermal conductivities and steam diffusion coefficients for the gas mixture which are 60% and 30% above those for a steam air mixture without Helium. The improved molecular transport resulting

from the presence of Helium enhances the heat transfer and condensation and explains why the steam addition in phase II that occurred nearly at the same rate as in test TH10 gave a slower than measured increase rate of the system pressure. It would be interesting to compare the current GASFLOW correlations for the calculation of the transport properties from the concentrations of the ternary mixture steam-Helium-air with those applied in other codes. The Helium concentration H1 in the upper plenum (see top of fig. 10) peaks at 35% at the end of phase I, which is 7% above the test data. There is agreement with the test data that no Helium gets into the annulus and to the lower plenum in phase I. Compared to the test, case A showed too little mixing of the Helium jet in phase I, which is also seen in predicted jet velocities at 2600 s that are 5 times higher than the measured data. The turbulent Helium diffusion is too weak due to the large aspect ratios of the narrow azimuthal and radial mesh cells around the Helium jet. But the vertical velocities calculated for the steam jet in phase II compared well with analytical results. Helium concentrations are diluted by the steam in phase II and get somewhat below the test data in the upper plenum. Some of the region with a higher Helium concentration is calculated to move to the sensor H2 in the upper annulus that is located under the Helium source by the circulation imposed from the steam plume. This leads to a slightly higher concentration at H2 relative to H1 which differs from the test data. In agreement with the test no Helium is calculated to reach the lower plenum in phase II and overall the Helium concentrations from the blind prediction are in fairly good agreement with the test data at the end of phase II. Only the pressure continues to stay somewhat below the measurement although a higher than measured steam rate was applied with the pre specified blind source.

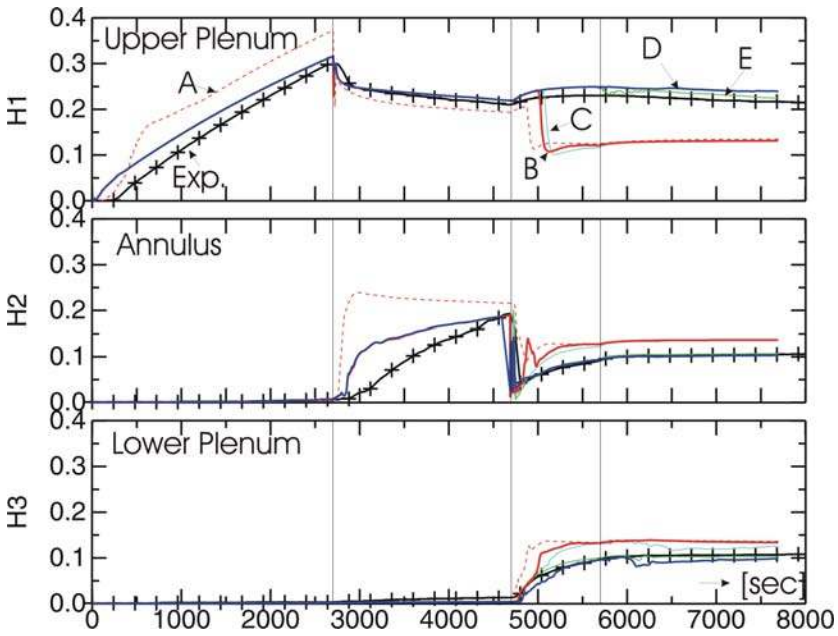

Figure 10: Helium concentrations from different GASFLOW simulations of test TH13

Cases B-E are post test calculations with the measured sources. They use a coarser radial and azimuthal mesh (fig. 9) similar to the one applied in case d of test TH10. They avoid the large aspect ratios which caused too little turbulent mixing of the Helium jet in phase I. The faces of the source cells for the vertical injection of steam and Helium are more than 10 times bigger with the coarser mesh than the real nozzle cross sections and due to the coarser mesh most of the vertical injection momentum is lost. The idea was that this will be outweighed by a stronger buoyancy that develops from the Helium and steam release. A small amount of steam was included in the Helium source which raised the pressure at the end of phase I to the measured value. The calculated pressure increase from the steam release in phase II approaches the measured transient quite well. The slight under prediction late in phase II would reduce if the fog generated by bulk condensation would be fully retained in the mixture and not rained out parametrically with the nominal rainout time constant of 10s used in the GASFLOW code. This rainout was necessary, though, because the accumulated fog den-

sity can lead to an instable gas mixing when the lighter steam is injected from below in phase III. Like in TH10 the use of the coarser mesh in cases B-E brought about a systematic increase of the pressure which is largely an effect of the applied wall functions. They shifted the pressure that was too low in case A to near the measured values. The much better aspect ratios in the coarser mesh also improved the prediction of turbulent Helium diffusion and the data for the Helium sensor H1 in the upper plenum approach the measured data quite well at the end of phase I. The impact of the steam injection in phase II on the Helium dilution is also better described with the coarser mesh in phase II so that the Helium sensors H1 and H2 nearly approach the measured data at the end of phase II (fig. 10).

Phases III and IV

The axial meshes in the blind case A and in case B were adjusted to match the injection area of the lower nozzle with the injecting faces of the source cells and simulate the radial injection in phase III with the correct injection velocity of 2.7 m/s. A summation of the positive flow rates over the inner cylinder and the annulus was performed at 5000 s at a height of 0.5 m above the lower end of the inner cylinder. It indicated in case A and B that 77% of the upward flow was calculated in the inner cylinder and 23% in the annulus. The central obstacle that had to be applied in both meshes for the time step reasons discussed before, imposed a flow area reduction in the inner cylinder of 18%. Separate test calculations only for phase III with and without the central obstacle give a slightly higher flow fraction through the inner cylinder. The additional flow area from removing the obstacle increased this fraction from 75 to 80% in these test cases. But the impact of the obstacle on the amount of steam entering the inner cylinder overall is weak. Our calculated fraction of 77% is confirmed by the CFX simulation of this experiment that was performed by NRG [7] and that demonstrated a quite similar splitting of the steam flow with 73% up flow in the inner cylinder. The scenario of phase III (fig. 11) calculated for cases A and B is quite similar with the scenarios that were calculated with other CFX simulations for this phase of the experiment. The lower steam release first compresses the stratified steam-Helium-air zone from phase II and pushes it above the inner cylinder into the plenum. The steam flowing up in the inner cylinder and the annulus spreads under the zone with lighter gas like a rising oil jet released deep under water when it reaches the water surface. Steam condensation occurs on the vessel wall. According to the calculation a circulation develops in the steam-air zone below. Figure 11 shows how the upper stratified zone with the Helium gets eroded from the shear flow induced by this circulation in case B and how the Helium is calculated to be mixed into the lower zone. Cases A and B predict that homogenization of the atmosphere in phase III occurs around 5000 s at the sensor in the upper plenum and that the whole atmosphere gets mixed from this circulation. The lower steam release in case B that starts from a correct pressure initially gives a faster than measured pressure increase. The pressure levels off when the steam leaving the inner cylinder condenses on the ves-

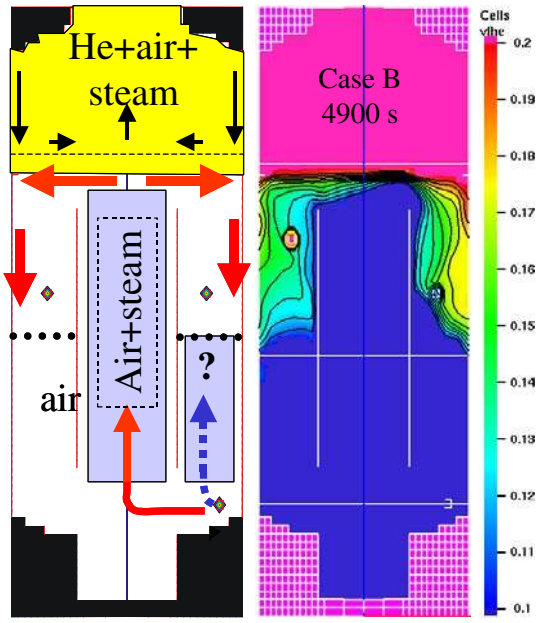

Figure 11: Predicted scenario for test TH13 with calculated Helium erosion in case B at 4900 s

sel. With the developing global circulation the pressure approaches the measured values at the end of phase III. The pressure decay below the test data in phase IV is related to the simulated fog rainout. Like in phase II rainout removes energy and leaving more fog in the atmosphere would reduce the pressure decay in phase IV and bring it in better agreement with the test data.

The scenario from the discussed CFD interpretations for phase III is not in agreement with the test data that show that the upper steam-Helium-air zone from phase II does not homogenize neither in phase III nor in phase IV. One potential reason was that a heavier gas region could have been built up by fog in the lower vessel from the fog formation around the initially cold nozzle in the lower plenum. We got an upper estimate for the fog content in the lower steam source that was not defined with the original source data [8]. It was used in all post test calculations cases B-E, however, the amount was too small for a sufficient reduction of the buoyancy from the lower steam release. A possibly more important reason can be seen from the comparison of the calculated and measured temperatures for case B shortly before the calculated onset of the homogenization at 5000 s in fig. 12. This figure compares the calculated and measured gas temperatures in the measuring plane between 120 and 300 degrees that is azimuthally offset to the lower source jet by 15 degrees. The measured thermocouple data

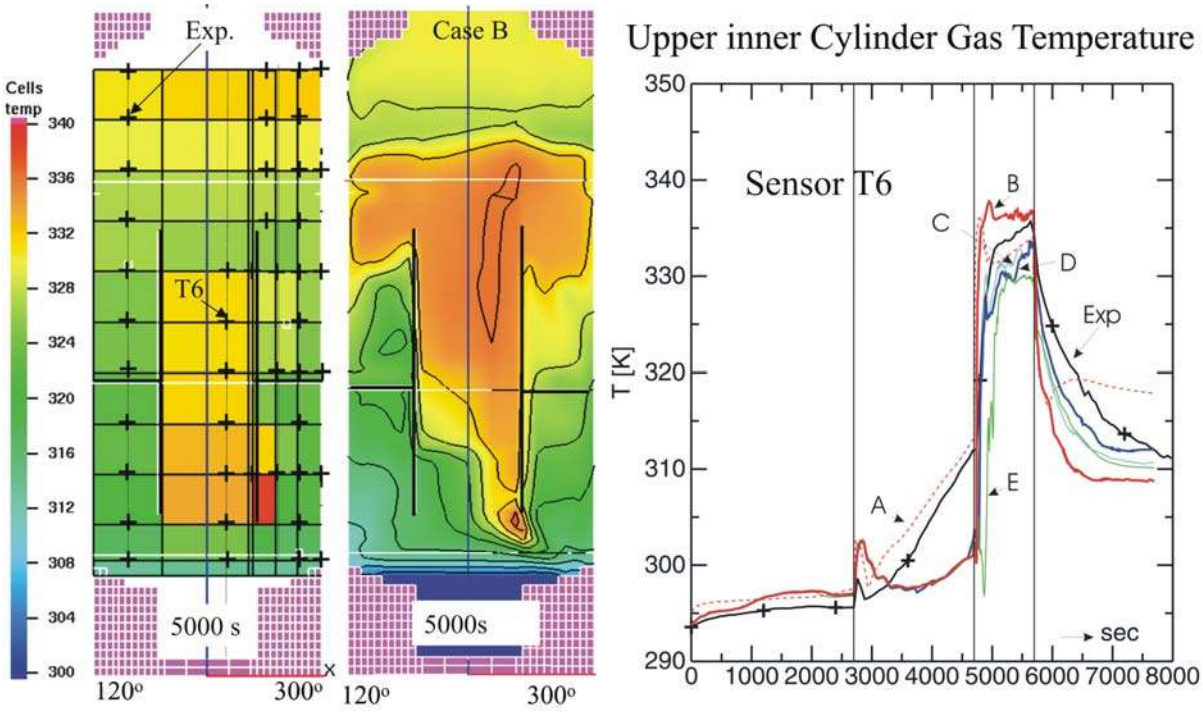

Figure 12: Temperature field at 5000 s and temperatures of sensor T6 in different simulations of test TH13

in this plane are displayed as enlarged cell data. The crosses mark the real sensor locations and are always put at the top of the cell that gives their reading (at the more narrow sensor locations the cells are defined to give the sensor location at their upper right hand corner). Cells with a cross at the top give un-interpolated sensor data. Cells without a cross at the top are interpretations with temperatures interpolated from horizontally adjacent sensors. The same color scaling is used in fig. 12 for the measured and calculated temperatures. Independent of the flow velocity which peaks higher in GASFLOW due to the central obstacle, the 77% fraction of the released steam that is calculated to rise in the inner

cylinder represents a certain energy flow that should find its correspondence in the measured gas temperatures. The fact that the measured temperatures are much lower than the calculated ones and that a large region with hot gas is predicted above the inner cylinder with this high flow fraction may indicate that in the experiment less flow occurred through the inner cylinder and that steam has found its way on a different path. The transient sensor output from cases A an B for the T6 thermocouple in the upper inner cylinder displays how these temperatures exceed the test data prior to the calculated homogenization of the atmosphere. The CFX calculations that were independently performed predict even higher temperatures than GASFLOW for these test conditions due to some other simplifications in the simulation.

Less up flow through the inner cylinder and/or a better mixing of the steam in the lower part of the vessel should bring about a less buoyant gas mixture which cannot attack the stratified layer above so much. This should reduce the erosion and mixing of the stratified gas layer. Our parametric investigations therefore assume a bypass of steam into the annulus with more mixing below the trays. More mixed steam in the annulus would also get in faster contact with the cold vessel below the trays and not allow for the calculated too rapid pressure buildup that results while the steam is rising through the inner cylinder without much possibility for condensation. The parametric cases C through E from table 2 investigated the impact of a different flow splitting between the inner cylinder and the annulus to find out necessary conditions for maintaining the stable stratification that was measured in phases III and IV. Case C applied a reduced radial injection velocity of 1.4 m/s by using a larger feed area for the radial injection. The flow fraction into the annulus increased from 23 to 81% due to this assumed reduction of the injection velocity. This also resulted in a reduced gas temperature for the sensor T6 in the upper inner cylinder that follows the measured temperature closely in the beginning of phase III (fig. 12). The steam in the annulus formed a narrow plume that rose on the outside of the inner cylin-

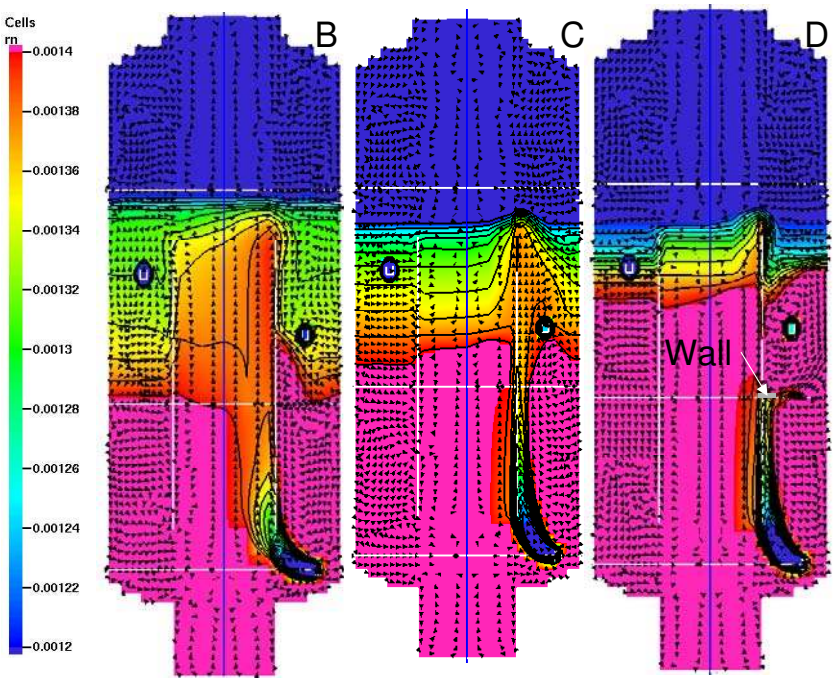

Figure 13: Macroscopic densities [g/cm3] and velocity fields at 5000s for test TH13 cases B, C, and D

der. It came up through the open slit above the source with little deflection on the trays and eroded the stratified layer together with the plume from the inner cylinder . The macroscopic densities which are

displayed in figure 13 together with the velocity vectors allow to compare the erosion of the lighter gas at 5000 s for the two cases B and C. Case C also predicts atmospheric homogenization from this erosion at the Helium sensor H1 in the upper plenum, it only occurs with a small delay over case B. The pressure rise in case C is similar to case B before the homogenization, but because of a reduced contact area with the upper vessel from the eccentrically rising plume the pressure continues to increase also during the atmospheric homogenization. Case D simulates a stronger mixing of the steam with air in the lower annulus. For this purpose a small impingement plate is inserted near the rising plume at the height of the condensate trays. Otherwise the geometric model of case C was used. Now the breaking of the plume in the annulus mixes it with heavier air and reduces its buoyancy. The freely rising plume from the flow fraction going up through the inner cylinder alone is too weak to break up the stratified layer in case D. The small impingement plate guides the rising steam towards the vessel wall. This gives an enhanced condensation that limits the pressure increase from the lower steam injection so that the pressure for case D nearly perfectly matches the test data through phase III. The deflection at the impingement plate also increases the vessel temperatures under the condensate trays and raises them nearer to the measured values. The Helium sensors H1-H3 in fig. 10 show a stable stratification for case D and also give excellent agreement with the test data for the H2 and H3 location in the annulus and lower plenum. The sensitivity study shows that a small deviation of the steam jet, for whatever reason, could influence the global He distribution in TH13 significantly. A similar stable stratification in phases III and IV is calculated by releasing all steam from phase III into the annulus. Case E simulated this event by releasing the steam over the face area of 5 azimuthal cells that cover an angle of 45 degrees thus giving it a negligible radial momentum. The widening of the source in case E gives a much larger entrainment area for the rising steam that reduces its buoyancy so that it cannot really attack the stratified layer anymore. It also gives a somewhat slower pressure increase which indicates that too much steam condensation would result below the trays when releasing 100% of the steam over a wide region in the lower annulus.

Conclusions

The ThAI test TH13 was defined as a 3D benchmark; it was the last of a series of tests to be analyzed within the new international standard problem ISP47 organized by the OECD. GASFLOW gives excellent predictions for the early part of this experiment. But it did not blindly predict the stable Helium stratification that was seen in the last part. The reason for the deviation in this special situation is not clear, because at decisive locations the measurement density was not high enough. It was decided to repeat this 3D experiment with an instrumentation that is tailored to answer the specific questions raised from CFD calculations. The good representation of the controlling phenomena in the full scale HDR containment test E11.2 with the ThAI test TH10 shows that these phenomena are only weakly dependent on scale. This gives confidence that the simulation of the condensation induced mixing in GASFLOW gives reliable predictions for full containment applications.

The experience gained from analyzing the discussed two containment experiments with different models can be summarized in a few points that may be helpful for the development of best practice guidelines for users of CFD codes. The calculations all show a certain dependency of the heat transfer and condensation on the applied near wall meshes that comes from the applied wall functions which can never represent the wide spectrum of free convection conditions occurring in different regions of the containment. But the calculated pressures approach the test data with an uncertainty band that is reasonable. To improve the prediction quality would require a more detailed resolution of the boundary layer by a local mesh refinement that is currently not feasible. Fog formation by bulk condensation impacts on the macroscopic density. The time constant for fog rainout and the minimum fog den-

sity that is assumed to be kept in the system have a certain impact also on the pressure and demonstrate that the treatment of fog and droplets in a separate flow field would be useful. Some sensitivity found from the mesh sizes near the walls should not overshadow the fact that there was little dependency within the applied variation of the mesh sizes inside the fluid. For the user the results show that it was important to avoid strong variations of the aspect ratios for certain phenomena like the turbulent diffusion of Helium. One may want to modify the solution algorithm in GASFLOW to implicitly determine the azimuthal diffusion which would allow the general use of cylindrical coordinates without having to insert central obstacles to avoid time step problems. The exact representation of the vertical injection momentum which can bring about small time steps was shown to be not necessary when the gas is injected into a heavier mixture because the experienced buoyancy often outweighs its injection momentum. For a horizontal buoyant jet the horizontal injection velocity must be exactly represented. For situations where numerical diffusion can become important the second order van Leer advection scheme should be activated.

References

[1] J. R. Travis, J. W. Spore, P. Royl et al.:"GASFLOW a computational fluid dynamics code for gases aerosols and combustion", FZKA-5994 Vol I-III, October 1998

[2] P. Royl, J. R. Travis, W. Breitung : „MODELLING AND VALIDATION OF CATALYTIC HYDROGEN RECOMBINATION IN THE 3D CFD CODE GASFLOW II", these proceedings

[3] P. Royl, J. R. Travis, W. Baumann, G. Necker : "ANALYSES OF CONTAINMENT EXPERIMENTS WITH GASFLOW II", procs. Nureth-10 Conference, Seoul, Korea, October 2003

[4] L. Wolf, H. Holzbauer: "Detailed Assessment of the HDR-hydrogen mixing experiments E11", Procs. Int. Conf. on New Trends in Nuclear System Thermohydraulics", Pisa, Italy, 1994

[5] P. Royl, J. R. Travis, E. A. Haytcher, and H. Wilkening, "Analysis of Mitigating Measures during Steam/Hydrogen distributions in Nuclear Reactor Containments with the 3D Field Code GASFLOW," presented at the OECD/NEA CSNI Workshop on the Implementation of Hydrogen Mitigation Techniques, Winnipeg, Canada, May 13–15, 1996

[6] U. J. Lee, P. Royl, J. R. Travis, T. Kanzleiter:" Blind 3D-Calculation of the Containment Thermal Hydraulic Test TH10 in the ThAI Facility Using GASFLOW II", Procs. Jahrestagung Kerntechnik Düsseldorf, May 25-27, 2004

[7] Houkema, M., Siccama, N. B.: "VALIDATION OF THE CFX-4 CFD CODE FOR CONTAINMENT THERMAL-HYDRAULICS", these proceedings

[8] S. Schwarz:" ThAI Experiment to ISP47, Thermodynamic Conditions of the Lower Steam Injection", e-mail to P. Royl from June 16, 2005

Acknowledgement

In addition to providing the test data Dr. T. Kanzleiter from Becker Technologies is acknowledged for giving further detailed informations on specific questions from the evaluation of our calculations. Dr.G. Grötzbach, FZK is acknowledged for his advice in interpreting the differences found between our calculations and the test data.